



# Timing of glacial retreat in the Wicklow Mountains, Ireland, conditioned by glacier size and topography

DOI:

[10.1002/jqs.3040](https://doi.org/10.1002/jqs.3040)

## Document Version

Accepted author manuscript

[Link to publication record in Manchester Research Explorer](#)

## Citation for published version (APA):

Tomkins, M., Dortch, J., Hughes, P., Huck, J., Tonkin, T., & Barr, I. (2018). Timing of glacial retreat in the Wicklow Mountains, Ireland, conditioned by glacier size and topography. *Journal of Quaternary Science*. <https://doi.org/10.1002/jqs.3040>

## Published in:

Journal of Quaternary Science

## Citing this paper

Please note that where the full-text provided on Manchester Research Explorer is the Author Accepted Manuscript or Proof version this may differ from the final Published version. If citing, it is advised that you check and use the publisher's definitive version.

## General rights

Copyright and moral rights for the publications made accessible in the Research Explorer are retained by the authors and/or other copyright owners and it is a condition of accessing publications that users recognise and abide by the legal requirements associated with these rights.

## Takedown policy

If you believe that this document breaches copyright please refer to the University of Manchester's Takedown Procedures [<http://man.ac.uk/04Y6Bo>] or contact [uml.scholarlycommunications@manchester.ac.uk](mailto:uml.scholarlycommunications@manchester.ac.uk) providing relevant details, so we can investigate your claim.



# 1 Timing of glacial retreat in the Wicklow Mountains, Ireland, 2 conditioned by glacier size and topography

3 Matt D. Tomkins\*, <sup>1</sup> Jason M. Dortch, <sup>2</sup> Philip D. Hughes, <sup>1</sup> Jonny J. Huck, <sup>1</sup> Toby N. Tonkin<sup>3</sup>  
4 and Iestyn D. Barr <sup>4</sup>

5 \*Corresponding author ([matthew.tomkins@postgrad.manchester.ac.uk](mailto:matthew.tomkins@postgrad.manchester.ac.uk))

6 <sup>1</sup>Department of Geography, School of Environment, Education and Development, The University of  
7 Manchester, Manchester, M13 9PL, UK

8 <sup>2</sup>Kentucky Geological Survey, 228 Mining and Mineral Resources Bldg., University of Kentucky,  
9 Lexington, KY 40506, USA

10 <sup>3</sup>Department of Natural Sciences, University of Derby, Kedleston Road, Derby, DE22 1GB, UK

11 <sup>4</sup>School of Science and the Environment, Manchester Metropolitan University, Chester Street,  
12 Manchester, M1 5GD, UK

## 14 Abstract

15 Reconstructing the deglacial history of palaeo-glaciers provides vital information on retreat  
16 processes; information which can inform predictions of the future behaviour of many of the world's  
17 glaciers. On this basis, this paper presents 170 Schmidt Hammer exposure ages from moraine  
18 boulders and glacially-sculpted bedrock to reveal the post-Last Glacial Maximum (LGM) history of  
19 the Wicklow Mountains, Ireland. These data suggest that large ice masses survived for 4-7 ka after  
20 retreat of the Irish Sea Ice Stream and were sustained by summit ice-fields until ~16.6 ka. Post-LGM  
21 retreat was driven by climate and involved numerous short-term ice front oscillations ( $\leq 1$  ka), with  
22 widespread moraine deposition during Heinrich Stadial 1. In contrast, marked asynchronicity in the  
23 timing of Younger Dryas deglaciation is closely linked to snow redistribution which demonstrates  
24 the sensitivity of small cirque glaciers ( $\leq 1$  km<sup>2</sup>) to local topography. This result has important  
25 implications for palaeoclimate reconstructions as cirque glacier dynamics may be (at least partly)  
26 decoupled from climate. This is further complicated by post-depositional processes which can result  
27 in moraine ages (e.g. <sup>10</sup>Be) which post-date retreat. Future palaeoclimate studies should prioritise  
28 cirques where snow contributing areas are small and where post-depositional disturbance of  
29 moraines is limited.

## 31 Keywords

- 32 • Schmidt Hammer exposure dating (SHED)
- 33 • Wicklow, Ireland
- 34 • Glacier chronology
- 35 • Topographic controls
- 36 • <sup>10</sup>Be dating

## 37 Introduction

38 Understanding how mountain scale ice-masses retreat is important if we are to predict the future  
39 behaviour of many of the world's glaciers. Fortunately, improvements in systematic and robust dating  
40 techniques and their application to glacial and glaciofluvial deposits mean that is now possible to gain  
41 vital information by reconstructing the retreat history of many of the world's former (palaeo) ice  
42 masses. In the British Isles, recent work has focused on understanding the dynamics of the Irish Ice  
43 Sheet (IIS) during the global Last Glacial Maximum (LGM; 23.3 – 27.5 ka; Hughes and Gibbard, 2015).  
44 This work has attempted to (1) establish the dimensions of the ice sheet at its maximum extent, (2)  
45 reveal the pattern and timing of retreat and (3) understand the configuration of the IIS within the  
46 larger British-Irish Ice Sheet (BIIS). With this in mind, recent studies have generated a wealth of  
47 geochronological data (e.g.  $^{10}\text{Be}$ ,  $^{36}\text{Cl}$ ,  $^{14}\text{C}$ ) to constrain the maximum extent of glaciation (e.g. Clark  
48 et al., 2009; Ballantyne and Stone, 2015; Barth et al., 2016), the timing of terrestrial and marine based  
49 ice sheet retreat (e.g. Sejrup et al., 2005; Clark et al., 2012), the dynamics of component ice caps and  
50 mountain glaciers (e.g. Ballantyne et al., 2006; Harrison et al., 2010; Barth et al., 2018) and the  
51 retreat history of the Irish Sea Ice Stream (ISIS) (e.g. Chiverrell et al., 2013; Smedley et al., 2017a), a  
52 major outlet of the BIIS (Smedley et al., 2017b). However, while considerable progress has been  
53 made, further work is necessary to understand the extent and retreat history of many mountain ice  
54 caps and glaciers in Ireland, particularly in areas where numerical ages are lacking, and to model their  
55 interaction with the IIS and marine based ice streams after the LGM. Understanding the fundamental  
56 climatic, topographic and glaciological processes which determine mountain glacier growth/decay, as  
57 revealed through reconstruction of retreat histories, provides critical information which can inform  
58 models of future glacier behaviour in response to anthropogenic forcing of climate.

59 In the Irish Sea Basin, ice caps centred on the mountains of Wales (Hughes et al., 2016), the Lake  
60 District (Wilson et al., 2013) and Wicklow, Ireland (Ballantyne et al., 2006) coalesced with the ISIS  
61 during the LGM and may have persisted after ISIS retreat. However, while the deglacial chronologies  
62 of the Welsh and Lake District ice caps are constrained by  $^{10}\text{Be}$ , OSL and  $^{14}\text{C}$  ages (Ballantyne et al.,  
63 2009; McCarroll et al., 2010; Glasser et al., 2012; Lloyd et al., 2013; Hughes et al., 2016; Smedley et  
64 al., 2017b), there is a paucity of geomorphological and geochronological evidence for post-LGM  
65 activity in the Wicklow Mountains.  $^{10}\text{Be}$  ages from summits in Wicklow (Ballantyne et al., 2006) and  
66 the adjacent Blackstairs Mountains (Ballantyne and Stone, 2015) indicate summit deglaciation soon  
67 after the LGM ( $n = 5$ ; 21.0 - 22.9 ka), while a single  $^{36}\text{Cl}$  age from the Mottee Stone, a large glacial  
68 erratic (~150 tonnes) transported ~13 km SE from its Wicklow source area, indicates separation of  
69 terrestrial ice and the ISIS by  $23.1 \pm 2.2$  ka (Bowen et al., 2002). This timeframe accords with  
70 Bayesian modelling of ice stream retreat, with the ISIS retreating ~80 km along the Irish coast during  
71 the interval 20.8 – 23.9 ka (Smedley et al., 2017b). Recent research has begun to establish the  
72 geomorphological context for deglaciation in the Wicklow Mountains (Knight et al., 2017). However,  
73 with the exception of isolated  $^{14}\text{C}$ ,  $^{36}\text{Cl}$  and  $^{10}\text{Be}$  ages from cirque moraines at Lough Nahanagan and  
74 Kelly's Lough (Colhoun and Synge, 1980; Bowen et al., 2002; Barth et al., 2018), the retreat history  
75 of the Wicklow Ice Cap is poorly constrained by numerical ages. To address this knowledge gap, this  
76 study presents 170 Schmidt Hammer (SH) exposure ages from cirque and valley moraines and from  
77 a summit overridden by ice at the LGM. These data provide (1) the first comprehensive retreat  
78 history for the Wicklow Ice Cap, (2) new information on the extent, timing and dynamics of Late  
79 Pleistocene mountain glaciation; information which complements a growing body of research in  
80 Ireland (e.g. Barth et al., 2016) and within the Irish Sea Basin (e.g. Hughes et al., 2016), and perhaps  
81 most significantly, (3) new insight into the climatic and topographic factors which conditioned post-  
82 LGM retreat.

## 83 Methods

84 To develop a deglacial chronology, sampling was focused on prominent moraines and boulder  
85 accumulations as these are the best geomorphological indicators of the dimensions of former  
86 mountain glaciers (Barr et al., 2017). Key sites along the main SW-NE axis of the mountain range  
87 were targeted for Schmidt Hammer exposure dating (SHED; Tomkins et al., 2016) including glacially-  
88 deposited boulders on prominent cirque moraines (>400 m) at Kelly's Lough (KL), Lough Nahanagan  
89 (LN), Mullaghcleevaun (MC) and Upper Lough Bray (ULB). Moraines targeted for SHED exhibit good  
90 spatial coherence (Kirkbride and Winkler, 2012) as they are generally matrix-poor, boulder-rich and  
91 feature clearly defined moraine crests, although the outer cirque moraine at Lough Nahanagan is  
92 degraded (Colhoun and Synge, 1980). This moraine is ~1 km in length, broadly convex in cross-  
93 profile form and consists of unsorted granite, sand and gravel deposits with entrained glacially  
94 smoothed granite boulders (1 - 4 m diameter; Colhoun and Synge, 1980). Multiple nested moraines  
95 and boulder accumulations are preserved within the inferred YD glacial limit at each site, which  
96 conforms to a pattern of active oscillatory retreat (Bickerdike et al., 2017). In addition, samples were  
97 obtained from valley moraines (250 – 400 m, c. 2 - 4 km from cirque headwalls) at Carrawaystick  
98 Brook (CB), Upper Glendasan (UGD), Lough Brook (LB) and Glenmacnass Waterfall (GW) and  
99 from ice-moulded bedrock and erratic boulders from the summit of Carrigshouk (CS; 571 m), which  
100 was overridden by ice at the LGM (Fig. 1; Table 1). 20 surfaces were sampled at each site  
101 (Carrawaystick Brook; n = 10) and 170 surfaces were sampled in total, comparable to previous  
102 applications of SHED in the Mourne Mountains, Northern Ireland (Barr et al., 2017).

103 30 R-values were generated per surface (Niedzielski et al., 2009). Sampled boulders were of  
104 sufficient size (> 25 kg; Sumner and Nel, 2002; Demirdag et al., 2009) and all sampled surfaces were  
105 free of surface discontinuities (Williams and Robinson, 1983) and lichen (Matthews and Owen, 2008).  
106 All sampled surfaces were quartz-rich, medium-coarse grained Caledonian granite (GSI, 2013;  
107 Bedrock Geology; Scale 1:500,000), with no clear spatial variability in grain size or rock composition.  
108 Although smaller scale geological maps indicate some variability between sampled sites (GSI, 2016;  
109 Bedrock Geology; Scale 1:100,000), the predominant style of weathering is sub-aerial, as evidenced  
110 by granular disintegration of the rock surface (André, 2002; Tomkins et al., 2018b). Although  
111 weathering rate variability cannot be excluded as an explanation for contrasting exposure age  
112 distributions across geological boundaries, it appears unlikely that these surfaces would weather at  
113 significantly different rates given their comparable grain size (1-5 mm), quartz content (~20%),  
114 degree of lichen colonisation and phenocryst size ( $\leq 30$  mm). Moreover, given the long-timescales of  
115 exposure ( $\geq 11$  ka) and limited climatic variability across the relatively small mountain range (~220  
116 km<sup>2</sup>), any differences in surface R-Values due to lithology will likely be significantly smaller than the  
117 effect of variable exposure age. This interpretation is supported by large spatial scale <sup>10</sup>Be-SH  
118 calibration curves from the British Isles (Tomkins et al., 2016; 2018a; n = 54; R<sup>2</sup> = 0.94, p < 0.01) and  
119 the Pyrenees (Tomkins et al., 2018b; n = 52; R<sup>2</sup> = 0.96, p < 0.01) which indicate that the primary  
120 control on surface R-Values is cumulative exposure to sub-aerial weathering. *Instrument calibration*  
121 (Correction Factor = 1.017) and *age calibration* (Correction Factor = 0.992) were performed using  
122 the SHED-Earth online calculator (<http://shed.earth>) following the recommendations of Dortch et al.  
123 (2016) and Tomkins et al. (2018a). SH exposure ages and 1σ uncertainties were calculated based on  
124 the arithmetic mean for each surface (Mean of 30 R-values) and based on the updated calibration  
125 curve of Tomkins et al. (2018a) which includes <sup>10</sup>Be dated surfaces from Blackstairs Mountain,  
126 Wexford (n = 2; Ballantyne and Stone, 2015) and Bloody Foreland, Donegal (n = 6; Ballantyne et al.,  
127 2007; Clark et al., 2009). These data fit the trend established at calibration sites in Scotland and NW

128 England and indicate that errors in SH exposure age estimates due to climatic variability appear  
129 unlikely (Barr et al., 2017). Calibration site exposure ages are calculated using the online calculators  
130 formerly known as the CRONUS-Earth online calculator (<http://hess.ess.washington.edu/math/>,  
131 Wrapper script 2.3, Main calculator 2.1, constants 2.3, muons 1.1; Balco et al., 2008) and are based  
132 on the time-dependent Lm scaling (Lal, 1991; Stone, 2000), the Loch Lomond Production Rate (LLPR;  
133 Fabel et al., 2012;  $4.02 \pm 0.18$  atoms  $\text{g}^{-1} \text{a}^{-1}$ ) and assuming 0 mm  $\text{ka}^{-1}$  erosion. The LLPR is  
134 constrained by independent  $^{14}\text{C}$  ages (MacLeod et al., 2011) and is the most widely used local  
135 production rate in the British Isles. However, the results presented here will be subject to  
136 recalibration in light of future refinement of local production rates. To ensure consistency when  
137 comparing the results of this study with independent numerical ages from Wicklow and other  
138 mountain massifs,  $^{10}\text{Be}$  ages from Ballantyne et al. (2006), McCarroll et al. (2010), Hughes et al.,  
139 (2016) and Barth et al. (2018) were recalibrated following the methods described above. Reported  
140  $^{36}\text{Cl}$  ages have not been recalibrated (Bowen et al., 2002; Ballantyne et al., 2009) due to incomplete  
141 sample information.

142 Reported SH exposure ages are interpreted to reflect the cumulative exposure of rock surfaces to  
143 sub-aerial weathering. Based on the assumption that sampled rock surfaces are glacial in origin e.g.  
144 boulders deposited on moraines or bedrock surfaces eroded sub-glacially, the onset of exposure can  
145 be considered contemporaneous with deglaciation. However, boulders can reside sub-aerially for  
146 considerable periods after glacial retreat (Hughes et al., 2016), leading to rock surface shielding,  
147 minimal sub-aerial weathering and higher Schmidt Hammer R-Values. These surfaces would generate  
148 SH exposure ages which post-date retreat and instead, likely reflect the timing of boulder  
149 exhumation and the stabilisation of the moraine ridge (Hallet and Putkonen, 1996). Given the  
150 growing consensus that moraine ages are more likely influenced by post-glacial instability than prior  
151 exposure (Heyman et al., 2011), the most cautious approach is to interpret SHED data as minimum  
152 limiting ages (Briner et al., 2005). The influence of prior exposure on surface R-Values is currently  
153 unclear, with limited data on the depth-dependence of sub-aerial weathering in granitic surfaces. For  
154  $^{10}\text{Be}$ , surface erosion of 3-5 m is necessary to remove the accumulated in-situ cosmogenic signal  
155 (Gosse and Phillips, 2001; Hughes et al., 2016; Briner et al., 2016). However, the depth of erosion  
156 required to 'reset' the surface for Schmidt Hammer testing is not known. If the required depth is  
157 comparable to  $^{10}\text{Be}$ , then is it possible that surfaces could retain a weathering signature from a  
158 previous period of exposure. While it is clear that further work is needed to address this  
159 uncertainty, and the uncertainty introduced by moraine stabilisation processes, these issues can be  
160 mitigated by collecting statistically large datasets and by analysing the distribution of calculated ages  
161 (e.g. Dortch et al., 2013; Murari et al., 2014) to identify outlier ages which are compromised by  
162 geological uncertainty. For each sampled site ( $n = 9$ ), probability density estimates (PDEs) were  
163 produced and modelled to separate out the highest probability Gaussian distribution (Fig. 2; Dortch  
164 et al., 2013). Using the KS density kernel in MATLAB (2015) and a dynamic smoothing window based  
165 on age uncertainty, PDE peaks and tails were separated into individual Gaussian distributions, the  
166 sum of which integrates to the cumulative PDE at 1000 iterations to obtain the best fit. The re-  
167 integrated PDE (made from the isolated Gaussians) goodness of fit is indicated graphically (Dortch et  
168 al., 2013). This analytical method has been employed in studies using  $^{10}\text{Be}$  (c.f. Dortch et al., 2013;  
169 Murari et al., 2014) to account for negative or positive skew of datasets and to identify ages that are  
170 too young (*moraine degradation*; Heyman et al., 2011) or too old, respectively (*inheritance*; Hallet and  
171 Putkonen, 1996). Full sample information for the 170 sampled surfaces sampled can be found in the  
172 Supplementary Dataset.

173 Based on the results of SHED, three dimensional reconstructions of cirque glaciers were generated  
174 using the GLaRe tool (Pellitero et al., 2016; Basal shear stress = 100 kPa; Step length = 10 m) and  
175 used to estimate palaeo equilibrium-line altitudes (ELAs). Valley glaciers were also reconstructed for  
176 individual catchments using this method although ELAs were not calculated for these ice  
177 configurations as geochronological data are not available for all glacier outlets. ELAs were estimated  
178 using the GIS tool of Pellitero et al. (2015), applying the area-altitude balance ratio method (AABR =  
179  $1.9 \pm 0.81$ ; Rea, 2009). ELAs are controlled by climate (Ohmura et al., 1992; Hughes and Braithwaite,  
180 2008) but are also strongly influenced by non-climatic factors (Table 2), such as the supply of snow  
181 and ice from indirect sources (Mitchell, 1996; Kern and Laszlo, 2010). To assess the impact of  
182 'redistributed' snow and ice, combined snow and avalanche contributing areas ( $A_c$ ) were calculated  
183 (c.f. Ballantyne, 2007a,b; Barr et al., 2017; Dominant wind direction W/SW = 210 - 300°, Avalanche  
184 slopes  $\geq 25^\circ$ ) and compared to total glacier surface areas ( $A_g$ ). The  $A_c/A_g$  ratio is a proxy for the  
185 potential contribution of redistributed snow to glacier accumulation.

186

## 187 Results

188 Gaussian exposure age distributions for each site (Table 1) are in correct stratigraphic order in  
189 individual glacier catchments, are broadly consistent with comparable deglacial chronologies across  
190 the British Isles (Clark et al., 2012), and clearly differentiate cirque and valley moraines, with  
191 deposition during the Younger Dryas (YD; 11.7 - 12.9 ka) and Oldest Dryas respectively (GS-2.1a;  
192 14.7 - 17.5 ka). Moreover, these datasets are chronologically robust (Kirkbride and Winkler, 2012),  
193 with well-dated moraine sequences in Glenmalur, Glendasan and Glenmacnass (Fig. 1), and provide a  
194 framework for a wider morphostratigraphic deglacial chronology for the Wicklow Mountains (Knight  
195 et al., 2017). At cirque sites, SHED indicates deglaciation by  $12.31 \pm 0.51$  ka at Upper Lough Bray,  
196  $12.00 \pm 0.44$  ka at Kelly's Lough  $11.40 \pm 0.13$  ka at Mullaghcleevaun and  $10.93 \pm 0.26$  ka for the  
197 outer moraine at Lough Nahanagan (Colhoun and Synge, 1980). In contrast, valley moraines were  
198 deposited at  $16.46 \pm 0.58$  ka at Glenmacnass Waterfall,  $16.21 \pm 0.60$  ka at Upper Glendasan,  $15.48 \pm$   
199  $0.35$  ka at Carrawaystick Brook and  $15.41 \pm 0.30$  ka at Lough Brook. Finally, SHED indicates the  
200 emergence of Carrigshouk by  $16.64 \pm 0.82$  ka. This date provides a minimum age for wider summit  
201 deglaciation in the Wicklows Mountains due to its comparatively low elevation (571 m) and central  
202 position on the range divide.

203 Independent radiometric ages from Lough Nahanagan ( $^{14}\text{C}$ ,  $^{36}\text{Cl}$ ,  $^{10}\text{Be}$ ) and Kelly's Lough ( $^{10}\text{Be}$ ) can  
204 be used to verify the results of SHED (Colhoun and Synge, 1980; Bowen et al., 2002; Barth et al.,  
205 2018). Unfortunately, geochronological data from Lough Nahanagan are clearly conflicting and  
206 indicate moraine deposition at either 11.5 - 11.6 ka ( $n = 2$ ;  $^{14}\text{C}$ ),  $17.9 \pm 1.0$  ka ( $n = 1$ ;  $^{36}\text{Cl}$ ) or  
207 between 9.7 - 21.7 ka ( $n = 3$ ;  $^{10}\text{Be}$ ). While the limited number of samples ( $n = 6$ ) prevents  
208 statistically robust identification and rejection of erroneous results (Tomkins et al., 2018b), and in  
209 turn, independent verification of SHED data at this site, the observed age scatter does highlight the  
210 importance of pre- or post-depositional processes at Lough Nahanagan, with uncertainty introduced  
211 by moraine stabilisation (Hallet and Putkonen, 1996), nuclide inheritance (Putkonen and Swanson,  
212 2003), or a combination of both. At Kelly's Lough,  $^{10}\text{Be}$  ages ( $n = 6$ ; Barth et al., 2018) are also likely  
213 influenced by geological uncertainty and are non-normally distributed, with ages of 9.5 - 9.7 ka ( $n =$   
214 2), 11.2 - 11.7 ka ( $n = 3$ ) and one outlier age of  $137 \pm 7$  ka. This 'old' outlier does not conform to  
215 the  $2\sigma$  test (Dortch et al., 2013) and matches the typical signature of nuclide inheritance observed in  
216 analysis of large  $^{10}\text{Be}$  datasets (Dortch et al., 2013; Murari et al., 2014). Excluding this outlier returns

217 a reduced dataset ( $n = 5$ ) with a mean age of  $10.6 \pm 0.5$  ka (Arithmetic mean  $\pm$  Standard Error of the  
218 Mean; SEM) following the analytical steps of Barth et al. (2018) and standard procedures for  
219 interpreting moraine age information i.e. the timing of deglaciation is determined as the mean of  
220 moraine boulder ages (Briner et al., 2005). However, this interpretation is based on the assumption  
221 of rapid moraine stabilisation after ice retreat. Moraine exposure ages (e.g.  $^{10}\text{Be}$ ) relate to the  
222 emplacement or exhumation of surfaces and the onset of exposure to cosmic radiation (Gosse and  
223 Phillips, 2001). In many geomorphological settings, these events may be contemporaneous with  
224 glacial retreat but not necessarily so (c.f. Hallet and Putkonen, 1996). Thus, the distribution of  
225 boulder ages on a single moraine more accurately represents the process of moraine stabilisation  
226 (Putkonen and Swanson, 2003) and individual ages are best interpreted as minimum-limiting ages  
227 (Briner et al., 2005). As a result, the greatest boulder age is hypothesised to most closely match the  
228 true age of a moraine, although only under an assumption of no prior exposure (Putkonen and  
229 Swanson, 2003). Based on this reasoning, the oldest ages from Kelly's Lough are likely more  
230 representative of the timing of deglaciation, with moraine deposition at  $11.44 \pm 0.12$  ka (Arithmetic  
231 mean of 3 oldest samples  $\pm$  SEM) or more conservatively, at  $11.65 \pm 0.74$  ka (Oldest sample; CRS-  
232 14-3; Barth et al., 2018). This interpretation is supported by PDE analysis ( $n = 5$ ; Dortch et al., 2013)  
233 which returns a peak Gaussian exposure age distribution of  $11.44 \pm 0.51$  ka. These estimates overlap  
234 within uncertainty with the SH Gaussian exposure age distribution of  $12.00 \pm 0.44$  ka (Fig. 2C) and  
235 confirm deglaciation during the late-YD or early Holocene. These independent  $^{10}\text{Be}$  ages join a  
236 growing body of evidence that SHED can generate accurate ages for glacial landforms (Rode and  
237 Kellerer-Pirklbauer, 2011; Ffoulkes and Harrison, 2014; Tomkins et al., 2016; 2018a; 2018b).

238 Reconstructed cirque glaciers (Table 2) range in size from  $0.35 \text{ km}^2$  (ULB) to  $1.10 \text{ km}^2$  (LN) while  
239 snow contributing areas ( $A_c$ ) range from  $0.12 \text{ km}^2$  (ULB) to  $1.07 \text{ km}^2$  (LN). At Lough Nahanagan and  
240 Mullaghcleevaun, extensive upland plateaus to the west and south ( $210 - 300^\circ$ ) account for large  
241 snow contributing areas ( $A_c \geq 1 \text{ km}^2$ ). In contrast, restricted upslope areas within the glacier  
242 drainage basin likely limited the potential for significant snow redistribution ( $A_c \leq 0.5 \text{ km}^2$ ) at Kelly's  
243 Lough and Upper Lough Bray. AABR ELAs for cirque glaciers range from 513 m (LN) to 648 m (KL)  
244 and show no clear spatial clustering. Finally, reconstructed valley glaciers range in size from  $4.96 \text{ km}^2$   
245 (UGD) to  $12.46 \text{ km}^2$  (GW) and demonstrate a progressive reduction in total glacier area ( $A_g$ )  
246 throughout the period 15.4 - 16.5 ka.

247

## 248 Discussion

249 Firstly, these data demonstrate that significant ice masses persisted in the Wicklow Mountains after  
250 the LGM, with large valley glaciers (Length:  $\sim 4$  km, Area:  $\sim 12.5 \text{ km}^2$ ) present until  $\sim 16.5$  ka; 4-7 ka  
251 after retreat of the ISIS (Smedley et al., 2017b). In contrast, lowland ( $23.1 \pm 2.2$  ka; Bowen et al.,  
252 2002) and summit deglaciation ( $n = 3$ ;  $21.0 - 21.9$  ka; Ballantyne et al., 2006) was coeval with ISIS  
253 retreat ( $20.8 - 23.9$  ka; Smedley et al., 2017b), SH exposure ages from the summit of Carrigshouk  
254 (571 m) indicate that summit ice fields were present on the range divide until  $16.64 \pm 0.82$  ka.  
255 However, distal summits were ice free as early as  $21.9 \pm 1.1$  ka (Djouce Mountain, 725 m),  $21.2 \pm$   
256  $1.1$  ka (Scarr, 641 m) and  $21.0 \pm 1.1$  ka (Kanturk, 523 m) and evidence a significant time lag in  
257 summit deglaciation ( $\sim 4.4$  ka). Collectively,  $^{10}\text{Be}$  and SHED ages indicate rapid downwastage of the  
258 Wicklow Ice Cap soon after the LGM and a transition to summit ice fields which sourced discrete  
259 outlet glaciers (e.g. Glenmacnass, Glendasan, Glenmalur; Fig. 1); some of which persisted until at  
260 least  $\sim 15.4$  ka and likely through until the onset of Greenland Interstadial I (GI-I; 12.9 - 14.7 ka;

261 Rasmussen et al., 2014). Deglaciation of Carrigshouk at ~16.6 ka marks a shift to topographically  
262 confined ice flow, with glaciers sourced from high elevation cirques, and likely reflects a time-  
263 progressive response to reduced moisture availability and winter aridity during this interval (Kelly et  
264 al., 2010).

265 This pattern of ice retreat, involving post-LGM downwastage of the ice cap and a transition to  
266 alpine-style valley glaciation, is consistent with numerical ages and geomorphological evidence from  
267 comparable mountain ice caps in the Irish Sea Basin and across Ireland. In Wales, summit  $^{10}\text{Be}$  ages  
268 record rapid and spatially uniform downwastage of the Welsh Ice Cap soon after the LGM, with  
269 summits ( $\geq 600$  m) exposed as nunataks at 19 - 20 ka (Hughes et al., 2016). This timeframe accords  
270 with summit  $^{10}\text{Be}$  ages from Wicklow (Ballantyne et al., 2006) and the Blackstairs Mountains  
271 (Ballantyne and Stone, 2015). However,  $^{14}\text{C}$  ages from proximal Welsh lowlands ( $15.82 \pm 0.39$  cal. ka  
272 BP; Lowe, 1981; Reimer et al., 2013) show that large alpine-style valley glaciers (Length: ~3.5 km),  
273 likely sourced from high elevation cirques, were present for ~4 ka after initial summit emergence  
274 (Hughes et al., 2016). This retreat history is matched by  $^{10}\text{Be}$  and  $^{36}\text{Cl}$  ages from the Lake District,  
275 which record substantial downwastage ( $< 750$  m) of the Lake District ice cap on the Scafell massif by  
276  $17.3 \pm 1.1$  ka ( $^{36}\text{Cl}$ ; Ballantyne et al., 2009). Despite this, a large valley glacier (Length: ~5 km),  
277 sourced from Scafell, was still present in Wasdale until  $16.7 \pm 0.9$  ka ( $^{10}\text{Be}$ ; McCarroll et al., 2010). In  
278 the central Lake District, a moraine age from Watendlath extends this period of alpine-style  
279 glaciation until  $15.2 \pm 0.9$  ka ( $^{10}\text{Be}$ ; Wilson et al., 2013). Collectively, these numerical ages show that  
280 while ice caps in the Irish Sea Basin underwent significant downwastage after the LGM, large valley  
281 glaciers persisted throughout the post-LGM period; likely until the onset of GI-1.

282 This pattern of ice retreat is also consistent with geomorphological evidence from the Kerry-Cork  
283 ice cap (KCIC) in SW Ireland (Ballantyne et al., 2007; Barth et al., 2016) although  $^{10}\text{Be}$  ages from  
284 cirque moraines in the Macgillycuddy's Reeks indicate that extensive (i.e., ice sheet and ice cap)  
285 glaciation had terminated by  $24.5 \pm 1.4$  ka (Barth et al., 2016). This timeframe is significantly earlier  
286 than comparable ice caps in Wicklow and throughout the Irish Sea Basin (Ballantyne et al., 2009;  
287 Hughes et al., 2016). However, cirque glaciers were present as recently as 16.7 - 16.9 ka ( $^{10}\text{Be}$ ;  $n = 2$ ;  
288 Harrison et al., 2010). While there is ongoing debate regarding the chronology of glaciation in SW  
289 Ireland (Barth et al., 2016; Knight, 2016) and the extent and configuration of the IIS and the KCIC  
290 during and after the LGM (Anderson et al., 1998; Rae et al., 2004; Harrison et al., 2010; Ballantyne et  
291 al., 2011), numerical ages from cirque moraines in the Macgillycuddy's Reeks (Harrison et al., 2010)  
292 support a prolonged period of post-LGM mountain glaciation, consistent with SHED,  $^{10}\text{Be}$ ,  $^{36}\text{Cl}$  and  
293  $^{14}\text{C}$  ages in other mountain massifs. These data support a period of renewed or continuous  
294 mountain glaciation after the LGM, with significant ice masses (Length:  $\leq 5$  km) recorded in the  
295 Wicklow Mountains at 15.4 - 16.5 ka, in Wales until  $15.82 \pm 0.39$  cal. ka BP (Lowe, 1981), in the  
296 Lake District at 15.2 - 16.7 ka (Ballantyne et al., 2009; Wilson et al., 2013) and in SW Ireland at 16.7  
297 - 16.9 ka (Harrison et al., 2010). These data represent a growing body evidence for substantial  
298 glaciation during the post-LGM period and support a model of gradual, oscillatory retreat of  
299 mountain glaciers after the LGM. Moreover, these numerical ages accord with wider evidence for  
300 post-LGM disintegration of the BISS into component ice caps (Clark et al., 2012).

301 Secondly, the geomorphological record indicates that post-LGM deglaciation involved numerous  
302 oscillations of glacier termini during the long-term retreat phase (~8 ka), with valley and cirque  
303 moraines deposited during the Oldest Dryas and Younger Dryas respectively (Fig. 2A). Correlative  
304 Gaussian exposure age distributions from valley moraines across the mountain range are indicative  
305 of a period of widespread moraine deposition, related to stabilisation or re-advance of valley glaciers



306 at 15.4 - 16.5 ka. Ice-marginal moraines provide direct evidence of former ice margin positions  
307 (Svendsen et al., 2004) but determining whether glaciers are stationary or re-advancing cannot be  
308 determined solely from moraine chronology. Moreover, while moraines can be used as indirect  
309 proxies for palaeoclimate (Benn and Ballantyne, 2005), a multitude of non-climatic factors can also  
310 influence patterns of moraine distribution, formation and preservation (Barr and Lovell, 2014), and  
311 therefore introduce complexity to links between periods of glacial deposition and wider climatic  
312 trends (Blaauw et al., 2007). However, the interval 15.4 - 16.5 ka is coeval with the peak ice rafted  
313 debris flux (Bard et al., 2000; Eynaud et al., 2009) and reduced sea surface temperatures (Bard et al.,  
314 2000) during Heinrich Stadial I (Fig. 2B; HSI) and the re-advance of the Irish Ice Sheet (IIS) and the  
315 ISIS during the Killard Point Stadial (~16 - 17.1 ka; McCabe et al., 2007; Clark et al., 2012). This  
316 period of glacier stabilisation or re-advance in Ireland during the Oldest Dryas was matched further  
317 down the North-East Atlantic margin in Spain (Palacios et al., 2017) and could reflect a direct  
318 response to North Atlantic climate perturbations (HSI) with short-term oscillations of the ice front  
319 ( $\leq 1$  ka) during the long-term post-LGM retreat phase. These chronological data match recent  
320 morphostratigraphic assessments of glacial geomorphology in the Wicklow Mountains which support  
321 a widespread pattern of sustained retreat interrupted by minor glacier readvance (Knight et al.,  
322 2017). Valley glacier retreat was synchronous across the Wicklow Mountains, as demonstrated by  
323 progressive deglaciation from low to high elevation (Fig. 3A;  $R^2 = 0.9116$ ;  $p = 0.045$ ). These data are  
324 indicative of climate-controlled retreat with independent outlet glaciers responding synchronously to  
325 reduced moisture availability (Kelly et al., 2010), irrespective of contrasting glacier aspects, source  
326 areas or glacier extents. Oldest Dryas valley glaciers were extensive ( $\leq 12.5$  km<sup>2</sup>), sustained by ice  
327 fields and prior to ~16.6 ka, overtopped low-lying summits (~571 m). As a result, the potential for  
328 significant redistribution of snow and avalanche material ( $A_c > A_g$ ) was limited, particularly during  
329 periods of winter aridity (Kelly et al., 2010). Therefore, while topography likely influenced the  
330 retreat pattern in individual valleys, post-LGM retreat (~15 - 17 ka) was primarily driven by climate.

331 In contrast, marked asynchronicity in the timing of final YD deglaciation (Fig. 3; 11.4 - 12.3 ka) is  
332 unrelated to cirque elevation (Fig. 3A;  $R^2 < 0.01$ ,  $p = 0.97$ ), palaeo-ELA (Fig. 3E;  $R^2 = 0.04$ ,  $p = 0.81$ )  
333 or site latitude ( $R^2 = 0.10$ ,  $p = 0.69$ ). If regional climate was the primary control on cirque glacier  
334 survival, then the timing of deglaciation would be expected to: (1) correlate with elevation, (2) be  
335 ELA dependent, or (3) show some relationship with temperature as a function of site latitude. These  
336 variables show little or negligible correlation with SH derived deglacial ages ( $R^2 \leq 0.1$ ) and are not  
337 statistically significant at  $p = 0.05$  ( $p \geq 0.69$ ). These data suggest that climate was not the dominant  
338 control on the timing of final YD deglaciation. Instead, glacier retreat was strongly controlled by  
339 local topography and the redistribution of wind-blown snow and avalanche material (Fig. 3B;  $R^2 >$   
340  $0.99$ ,  $p < 0.01$ ). Combined snow and avalanche contributing areas ( $A_c$ ) range from just 0.119 km<sup>2</sup> at  
341 Upper Lough Bray to 1.071 km<sup>2</sup> at Lough Nahanagan. For glaciers with large  $A_c$  areas, topography  
342 may exert the primary control on glacier formation and survival, and may account for the  
343 comparatively late-deglaciation of Lough Nahanagan and Mullaghcleevaun during the early-Holocene.  
344 By comparison, glaciers with small  $A_c$  areas, where the potential for redistribution of snow and  
345 avalanche material is limited, may respond quasi-synchronously to climate warming. For example, the  
346 early deglaciation of Upper Lough Bray at  $12.31 \pm 0.51$  ka is coeval with a gradual rise in summer air  
347 temperatures after ~12.5 ka (Brooks and Birks, 2000) which was likely sufficient to raise the 'climatic'  
348 ELA above cirque elevations ( $A_c/A_g = 0$ ; Barr et al., 2017) and initiate mass wastage. In contrast,  
349 abundant snow redistribution ( $A_c \geq 1$ ), conditioned by existing topographic configurations (extensive  
350 upland plateaus), was likely sufficient to locally suppress the 'local' (non-climatic) ELA and promote  
351 glacier survival at other sites. However, the contribution of redistributed snow to glacier

352 accumulation almost certainly diminished throughout the YD as summer air temperatures increased  
353 rapidly towards the onset of the Holocene (Brooks and Birks, 2000), thus limiting snowpack  
354 preservation. These data indicate that while regional climate provides the baseline conditions for  
355 glacier growth and decay, cirque glacier oscillations may primarily reflect the influence of topography.  
356 In this scenario, macro-topographic configurations condition glaciers to be sensitive to cold and/or  
357 wet climate and provide a first-order control on glaciation by (1) facilitating glacier initiation, and (2)  
358 enabling a lagged response to warming climate.

359 However, there is a weak correlation between glacier size ( $A_g$ ) and deglaciation age (Fig. 3C;  $R^2 =$   
360  $0.77$ ,  $p = 0.12$ ), although the size variation between the smallest (ULB;  $0.35 \text{ km}^2$ ) and largest  
361 reconstructed glacier (LN:  $1.10 \text{ km}^2$ ) is minimal ( $\sim 0.75 \text{ km}^2$ ). As such, significant within-mountain  
362 range variation in glacier response times is not anticipated (Raper and Braithwaite, 2009). This may  
363 account for the weak correlation between  $A_c/A_g$  ratios and deglaciation ages (Fig. 3D;  $R^2 = 0.58$ ,  $p =$   
364  $0.24$ ) although the observable trend demonstrates the probability of early deglaciation for glaciers  
365 with small  $A_c/A_g$  ratios. Based on this reasoning, we conclude that for small YD glaciers, local  
366 topoclimatic controls can be more significant than wider regional climate in determining cirque  
367 glacier functioning, and in particular, the timing of final deglaciation. Avalanches accumulation area  
368 and deglaciation age correlations have important implications for palaeoclimate reconstructions  
369 based on dating of cirque moraines (e.g. using  $^{10}\text{Be}$  or SHED), as cirque glacier ELAs can be non-  
370 representative of the regional climate and consequently glacier dynamics are likely to be decoupled  
371 from climatic changes occurring in the North Atlantic region. This phenomenon is observed today in  
372 the behaviour of small glaciers in marginal glaciated settings such as the Italian Alps (Colucci, 2016)  
373 and other Mediterranean mountains (Hughes, 2018), which demonstrates the sensitivity of glaciers  
374 to macro-topography (Mitchell, 1996; Allen, 1998; Benn and Lehmkuhl, 2000; García-Ruiz et al., 2000;  
375 López-Moreno et al., 2006a, 2006b; Kern and Laszlo, 2010), particularly in marginal glaciated regions  
376 (Chueca and Julián, 2004; Mills et al., 2009). These data from Ireland also show that the impact of  
377 topography on glacier functioning is most significant when glaciers are small ( $\leq 1 \text{ km}^2$ ), resulting in  
378 clear asynchronicity in deglaciation (Fig. 3A;  $R^2 = < 0.01$ ), and provide further evidence that the  
379 climatic integrity of cirque glaciers may be limited (Kirkbride and Winkler, 2012). In contrast, large  
380 glaciers ( $\sim 12.5 \text{ km}^2$ ), with limited potential for snow redistribution, have been shown to respond  
381 synchronously to climate forcing (Fig. 3A;  $R^2 = 0.9116$ ). Modelling studies have shown that  
382 topoclimatic variables (solar radiation/snow redistribution) can predict the style of deglaciation  
383 (moraine distribution) for small Younger Dryas glaciers (Coleman et al., 2009; Bickerdike et al.,  
384 2017). The chronological data presented here provides new evidence that topographic controls not  
385 only influence the style of deglaciation, but can determine the timing of final deglaciation, with clear  
386 within-mountain range variability.

387 A further challenge in linking cirque glacier oscillations to climatic fluctuations is the potential impact  
388 of moraine stabilisation (Hallet and Putkonen, 1996). This post-depositional process can result in  
389 moraine ages (e.g.  $^{10}\text{Be}$ , SHED) which post-date glacial retreat. A 1-2 ka early stabilization period has  
390 been recorded for Alpine moraine sequences in Alaska and the Alps (Briner et al., 2005; Ivy-Ochs et  
391 al., 2006, 2008; Dortch et al., 2010a). In high-mountain and alpine environments, glaciers can  
392 produce distinctive asymmetric ice-contact fans that undergo rapid gullying and post-depositional  
393 reworking on their ice-proximal slopes (e.g. Hambrey et al., 2008; Lukas et al., 2012). However,  
394 these landforms are topographically and sedimentologically distinct from the low-relief,  
395 topographically concordant valley and cirque landsystems found in the Wicklow Mountains.  
396 Moreover, there has been comparatively little attention on the processes of moraine development in  
397 these low-relief environments, with analogue studies predominantly focused on 'hummocky moraine'

398 landsystems (e.g. Benn and Lukas, 2006). In addition, there has been a relative paucity of research  
399 into moraine processes in smaller cirque type landsystems, likely under the assumption of rapid  
400 stabilisation after deglaciation. Recent work has highlighted the importance of self-censoring in  
401 cirque and valley environments due to oblitative overlap (Barr and Lovell, 2014) or ice-cored  
402 moraine degradation (Crump et al., 2017; Tonkin et al., 2017), while external-censoring due to slope  
403 instability may also provide a control on moraine stabilisation (Barr and Lovell, 2014). As a result,  
404 there is considerable uncertainty regarding the robustness of chronological datasets for cirque  
405 moraine systems (Kirkbride and Winkler, 2012).

406 To produce better-resolved glacier chronologies, researchers can account for moraine stabilisation  
407 through (1) morphostratigraphic comparison of moraine sequences, (2) Gaussian separation of  
408 exposure ages (Dortch et al., 2013), (3) assessment against independent geochronological data (e.g.  
409  $^{14}\text{C}$ ) and (4) consideration of modern process studies and likely modern analogues for moraine  
410 assemblages when assessing site suitability for a give geochronological approach (e.g. Çiner et al.  
411 2015). Based on these criteria, we infer that moraine stabilisation may be a key post-depositional  
412 process for the outer moraine at Lough Nahanagan. Firstly, this moraine is degraded (Colhoun and  
413 Synge, 1980) and is morphologically distinct from sampled cirque moraines at Mullaghcleevaun,  
414 Kelly's Lough and Upper Lough Bray which are tall ( $> 3$  m), matrix-poor, boulder-rich, and feature  
415 clearly defined moraine crests (Fig. 4). The morphology of these large terminal moraines likely  
416 reflects the incorporation of Lateglacial rock slope failure (RSF) debris (Ballantyne et al., 2013). This  
417 debris may account for a significant proportion of the sediment budget of YD glaciers, particularly in  
418 cirques characterised by steep headwalls where RSF activity is enhanced.

419 Secondly, Gaussian separation of SHED data for Lough Nahanagan ( $n = 20$ ) reveals a clear 'two-peak'  
420 probability density function (Fig. 2C), with Gaussian exposure age distributions of  $10.93 \pm 0.26$  ka ( $n$   
421  $= 9$ ) and  $11.38 \pm 0.26$  ka ( $n = 9$ ). The youngest age post-dates the YD by  $\sim 0.8$  ka and is inconsistent  
422 with wider evidence for deglaciation of the British Isles by the YD/Holocene transition (MacLeod et  
423 al., 2011) although in isolation, this observation is insufficient to reject this age at this stage. In  
424 addition, this method highlights clear outlier ages ( $n = 3$ ; 12.8 - 13.5 ka). These Gaussian  
425 distributions can be rejected as they are comprised of fewer than 3 ages (c.f. Fig. 3 in Dortch et al.,  
426 2013). Independent  $^{14}\text{C}$  ages indicate deglaciation during the late YD and early Holocene (11.5 - 11.6  
427 ka; Colhoun and Synge, 1980) while a single  $^{36}\text{Cl}$  age suggests ice free conditions since  $17.9 \pm 1.0$  ka  
428 (Bowen et al., 2002), although this age likely reflects prior exposure (*inheritance*) and is rejected from  
429 further analysis. New  $^{10}\text{Be}$  ages from the outer moraine at Lough Nahanagan (Barth et al., 2018) are  
430 not internally consistent ( $n = 3$ ; 9.7 - 21.7 ka) and are inconclusive with regards to the timing of  
431 deglaciation at this site. Based on these data, we conclude that the older Gaussian exposure age  
432 distribution of  $11.38 \pm 0.26$  ka is more representative of final deglaciation as this age is consistent  
433 with previous  $^{14}\text{C}$  ages and accounts for both the distinctive geomorphological assemblage at this site  
434 and the clear 'two-peak' distribution of SHED ages. This conclusion indicates that moraine  
435 stabilisation and boulder exhumation may account for the degraded moraine surface and  
436 comparatively 'young' SHED ages.

437 These data provide further evidence that moraine ages are more likely influenced by post-glacial  
438 instability than prior exposure (Shanahan and Zreda 2000; Putkonen and Swanson 2003; Zech et al.  
439 2005; Heyman et al. 2011; Applegate et al., 2012). As a result, the growth or decay of small cirque  
440 glaciers ( $< 1$  km<sup>2</sup>), as determined by radiometric methods ( $^{10}\text{Be}$ ), may not only primarily reflect  
441 topographic controls, but may be profoundly influenced by post-depositional processes. The post-  
442 depositional evolution of YD moraine systems is largely unexplored at present and a clear co-benefit

443 of the SHED approach is the insight it provides into these processes; insight that is not readily  
444 afforded by other geochronological approaches. Future research should carefully consider landform  
445 context (Barr and Lovell, 2014) and prioritise sampling of cirque environments where snow and  
446 avalanche contributing areas ( $A_c$ ) are small (Warren, 1991; Mills et al., 2012; Barr and Lovell, 2014),  
447 where postglacial erosion is limited and where short transport distances promote the formation of  
448 matrix-poor boulder-rich moraines (Fig. 5; Pallàs et al., 2010). In these environments, snow  
449 redistribution is limited and moraines are more likely to stabilise rapidly after deglaciation. As such,  
450 these glaciers may respond quasi-synchronously to climatic fluctuations and may produce more  
451 robust palaeoclimatic reconstructions.

452

## 453 Conclusions

454 This study provides the first comprehensive glacial retreat history for the Wicklow Mountains,  
455 Ireland. 170 Schmidt Hammer exposure ages from cirque and valley moraines and from a summit  
456 overridden by ice at the LGM demonstrate that significant ice masses persisted for 4-7 ka after  
457 retreat of the Irish Sea Ice Stream and were sustained by summit ice-fields until ~16.6 ka. Post-LGM  
458 retreat involved numerous oscillations of glacier termini during the retreat phase, with widespread  
459 moraine deposition related to stabilisation or re-advance of valley glaciers during the Oldest Dryas,  
460 potentially in response to cooling during Heinrich Stadial I (HS1). However, these moraines reflect  
461 short-term oscillations ( $\leq 1$  ka) of the ice front during the long-term retreat phase (~8 ka), which  
462 was driven by reduced moisture availability and winter aridity. These data match numerical ages  
463 ( $^{10}\text{Be}$ ,  $^{36}\text{Cl}$ ,  $^{14}\text{C}$ ) from comparable mountain caps at the margins of the Irish Sea basin and in SW  
464 Ireland which support a model of widespread and persistent alpine glaciation during the post-LGM  
465 period. Significant ice masses (Length:  $\leq 5$  km) were present until the onset of Greenland Interstadial  
466 I and in some mountain massifs, for up to ~4 ka after initial summit emergence following the LGM.  
467 Valley glacier retreat in the Wicklow Mountains was driven by climate, with time-progressive  
468 deglaciation from low to high elevation ( $R^2 = 0.9116$ ). In contrast, marked asynchronicity in the  
469 timing of Younger Dryas (YD) deglaciation (11.4 - 12.3 ka), unrelated to site elevation, latitude or  
470 equilibrium line altitude (ELA), is accounted for by macro-topography and the redistribution of snow  
471 and avalanche material, sufficient to locally suppress the 'local' (non-climatic) ELA and promote glacier  
472 survival. Contrasting synchronicity in the timing of glacial retreat during these periods is conditioned  
473 by glacier size, with small YD glaciers ( $< 1$  km<sup>2</sup>) highly sensitive to local topographic controls. This  
474 result has important implications for palaeoclimate reconstructions based on dating of cirque  
475 moraines (e.g.  $^{10}\text{Be}$ , SHED), as cirque glacier dynamics may be (at least partly) decoupled from  
476 climate. This is further complicated by post-depositional processes which can result in ages which  
477 post-date retreat. As a result, future palaeoclimate reconstructions should prioritise cirques where  
478 snow and avalanche contributing areas ( $A_c$ ) are small and where the potential for post-depositional  
479 disturbance is limited (matrix-poor, boulder rich moraines).

480

## 481 Acknowledgements

482 MT is funded by a University of Manchester Presidents Doctoral Scholarship. Fieldwork was funded  
483 by the University of Manchester School of Environment, Education and Development Fieldwork  
484 Support Fund. JMD, PDH, and JJH would like to thank the University of Manchester Research  
485 Stimulation Fund. We would like to thank David Tomkins for fieldwork support and John and

486 Deirdre Lynham for their advice and hospitality. Thanks also go to Dr. Derek Fabel for kindly  
487 providing unpublished calibration data for the LLPR and to two anonymous reviewers for their  
488 constructive reviews which greatly improved this manuscript.

489

## 490 References

- 491 Allen TR. 1998. Topographic context of glaciers and perennial snowfields, Glacier National Park,  
492 Montana. *Geomorphology* **21**: 2017-216.
- 493 Anderson E, Harrison S, Passmore DG, Mighall, T. 1998. Evidence for Younger Dryas glaciation in  
494 the Macgillycuddy's Reeks, southwest Ireland. *Quaternary Proceedings* **6**: 75-90.
- 495 André MF. 2002. Rates of postglacial rock weathering on glacially scoured outcrops (Abisko-  
496 Riksgränsen Area, 68°N). *Geografiska Annaler, Series A: Physical Geography* **84**: 139-150.
- 497 Applegate PJ, Urban NM, Keller K, Lowell T V, Laabs BJC, Kelly MA, Alley RB. 2012. Improved  
498 moraine age interpretations through explicit matching of geomorphic process models to cosmogenic  
499 nuclide measurements from single landforms. *Quaternary Research* **77**: 293-304.
- 500 Balco G, Stone JO, Lifton NA, Dunai TJ. 2008. A complete and easily accessible means of calculating  
501 surface exposure ages or erosion rates from <sup>10</sup>Be and <sup>26</sup>Al measurements. *Quaternary Geochronology*  
502 **3**: 174-195.
- 503 Ballantyne CK. 2007a. Loch Lomond Stadial glaciers in North Harris, Outer Hebrides, North-West  
504 Scotland: glacier reconstruction and palaeoclimatic implications. *Quaternary Science Reviews* **26**: 3134-  
505 3149.
- 506 Ballantyne CK. 2007b. The Loch Lomond Readvance on north Arran, Scotland: glacier  
507 reconstruction and palaeoclimatic implications. *Journal of Quaternary Science* **22**: 343-359.
- 508 Ballantyne CK, McCarroll D, Stone JO. 2006. Vertical dimensions and age of the Wicklow Mountains  
509 ice dome, Eastern Ireland, and implications for the extent of the last Irish Ice Sheet. *Quaternary*  
510 *Science Reviews* **25**: 2048-2058.
- 511 Ballantyne CK, McCarroll D, Stone JO. 2007. The Donegal ice dome, northwest Ireland: dimensions  
512 and chronology. *Journal of Quaternary Science* **22**: 773-783.
- 513 Ballantyne CK, Stone JO. 2015. Trimlines, blockfields and the vertical extent of the last ice sheet in  
514 southern Ireland. *Boreas* **44**: 277-287.
- 515 Ballantyne CK, Stone JO, Fifield LK. 2009. Glaciation and deglaciation of the SW Lake District,  
516 England: implications of cosmogenic <sup>36</sup>Cl exposure dating. *Proceedings of the Geologists' Association* **120**:  
517 139-144.
- 518 Ballantyne CK, Wilson P, Gheorghiu D, Rodés, À. 2013. Enhanced rock-slope failure following ice-  
519 sheet deglaciation: timing and causes. *Earth Surface Processes and Landforms* **39**: 900-913.
- 520 Bard E, Rostek F, Turon J, Gendreau S. 2000. Hydrological Impact of Heinrich Events in the  
521 Subtropical Northeast Atlantic. *Science* **289**: 1321-1324.
- 522 Barr ID, Lovell H. 2014. A review of topographic controls on moraine distribution. *Geomorphology*  
523 **226**: 44-64.

- 524 Barr ID, Roberson S, Flood R, Dortch J. 2017. Younger Dryas glaciers and climate in the Mourne  
525 Mountains, Northern Ireland. *Journal of Quaternary Science* **32**: 104–115.
- 526 Barth AM, Clark PU, Clark J, McCabe AM, Caffee M. 2016. Last Glacial Maximum cirque glaciation  
527 in Ireland and implications for reconstructions of the Irish Ice Sheet. *Quaternary Science Reviews* **141**:  
528 85-93.
- 529 Barth AM, Clark PU, Clark J, Roe GH, Marcott SA, McCabe AM, Caffee MW, He F, Cuzzone JK,  
530 Dunlop, P. 2018. Persistent millennial-scale glacier fluctuations in Ireland between 24 ka and 10 ka.  
531 *Geology* **46**: 151-154.
- 532 Benn DI, Lehmkuhl F. 2000. Mass balance and equilibrium-line altitudes of glaciers in high-mountain  
533 environments. *Quaternary International* **65-66**: 15-29.
- 534 Benn DI, Ballantyne CK. 2005. Palaeoclimate reconstruction from Loch Lomond Readvance glaciers  
535 in the West Drumochter Hills, Scotland. *Journal of Quaternary Science* **20(6)**: 577-592.
- 536 Benn DI, Lukas S. 2006. Younger Dryas glacial landsystems in North West Scotland: an assessment  
537 of modern analogues and palaeoclimatic implications. *Quaternary Science Reviews* **25**: 2390–2408.
- 538 Bickerdike HL, Ó Cofaigh C, Evans DJA, Stokes CR. 2017. Glacial landsystems, retreat dynamics and  
539 controls on Loch Lomond Stadial (Younger Dryas) glaciation in Britain. *Boreas*.
- 540 Birks HJB. 2001. Chironomid-inferred Late-glacial air temperatures at Whitrig Bog, southeast  
541 Scotland. *Journal of Quaternary Science* **15**: 759–764.
- 542 Blaauw M, Bakker R, Christen JA, Hall VA, van der Plicht J. 2007. A Bayesian framework for age  
543 modeling of radiocarbon-dated peat deposits: Case studies from the Netherlands. *Radiocarbon* **49**:  
544 357-367.
- 545 Bowen DQ, Phillips FM, McCabe AM, Knutz PC, Sykes GA. 2002. New data for the Last Glacial  
546 Maximum in Great Britain and Ireland. *Quaternary Science Reviews* **21**: 89–101.
- 547 Briner JP, Kaufman DS, Manley WF, Finkel RC, Caffee MW. 2005. Cosmogenic exposure dating of  
548 late Pleistocene moraine stabilization in Alaska. *GSA Bulletin* **117**: 1108–1120.
- 549 Briner JP, Goehring BM, Mangerud J, Svendsen JI. 2016. The deep accumulation of <sup>10</sup>Be at Utsira,  
550 southwestern Norway: Implications for cosmogenic nuclide exposure dating in peripheral ice sheet  
551 landscapes. *Geophysical Research Letters* **43**: 9121–9129.
- 552 Chiverrell RC, Thrasher IANM, Thomas GSP, Lang A, Scourse JD, Van Landeghem KJJ, McCarroll D,  
553 Clark CD, Ó Cofaigh C, Evans DJA, Ballantyne CK. 2013. Bayesian modelling the retreat of the Irish  
554 Sea Ice Stream. *Journal of Quaternary Science* **28**: 200–209.
- 555 Chueca J, Julián A. 2004. Relationship between Solar Radiation and the Development and  
556 Morphology of Small Cirque Glaciers (Maladeta Mountain Massif, Central Pyrenees, Spain).  
557 *Geografiska Annaler. Series A, Physical Geography* **86**: 81-89.
- 558 Çiner A, Sarıkaya MA, Yıldırım C. 2015. Late Pleistocene piedmont glaciations in the Eastern  
559 Mediterranean; insights from cosmogenic <sup>36</sup>Cl dating of hummocky moraines in southern Turkey.  
560 *Quaternary Science Reviews* **116**: 44–56.
- 561 Clark J, Cabe AMMC, Schnabel C, Clark PU, Freeman S, Maden C, Xu S. 2009. <sup>10</sup>Be chronology of  
562 the last deglaciation of County Donegal, northwestern Ireland. *Boreas* **38**: 111–118.

- 563 Clark CD, Ely JC, Greenwood SL, Hughes ALC, Meehan R, Barr ID, Bateman MD, Bradwell T,  
564 Doole J, Evans DJA, Jordan CJ, Monteys X, Pellicer XM, Sheehy M. 2017. BRITICE Glacial Map,  
565 version 2: a map and GIS database of glacial landforms of the last British-Irish Ice Sheet. *Boreas*.
- 566 Clark CD, Hughes ALC, Greenwood SL, Jordan C, Sejrup HP. 2012. Pattern and timing of retreat of  
567 the last British-Irish Ice Sheet. *Quaternary Science Reviews* **44**: 112–146.
- 568 Coleman CG, Carr SJ, Parker AG. 2009. Modelling topoclimatic controls on palaeoglaciers:  
569 implications for inferring palaeoclimate from geomorphic evidence. *Quaternary Science Reviews* **28**:  
570 249–259.
- 571 Colhoun EA, Synge MF. 1980. The Cirque Moraines at Lough Nahanagan, County Wicklow, Ireland.  
572 *Proceedings of the Royal Irish Academy. Section B: Biological, Geological, and Chemical Science* **80**: 25–45.
- 573 Colucci RR. 2016. Geomorphic influence on small glacier response to post-Little Ice Age climate  
574 warming: Julian Alps, Europe. *Earth Surface Processes and Landforms* **41**: 1227–1240.
- 575 Crump SE, Anderson LS, Miller GH, Anderson RS. 2017. Interpreting exposure ages from ice-cored  
576 moraines: a Neoglacial case study on Baffin Island, Arctic Canada. *Journal of Quaternary Science* **32**:  
577 1049–1062.
- 578 Demirdag S, Yavuz H, Altindag R. 2009. The effect of sample size on Schmidt rebound hardness  
579 value of rocks. *International Journal of Rock Mechanics and Mining Sciences* **46**: 725–730.
- 580 Dortch JM, Hughes PD, Tomkins MD. 2016. Schmidt hammer exposure dating (SHED): Calibration  
581 boulder of Tomkins et al. (2016). *Quaternary Geochronology* **35**: 67–68.
- 582 Dortch JM, Owen LA, Caffee MW. 2013. Timing and climatic drivers for glaciation across semi-arid  
583 western Himalayan-Tibetan orogen. *Quaternary Science Reviews* **78**: 188–208.
- 584 Dortch JM, Owen LA, Caffee MW, Brease P. 2010. Late Quaternary glaciation and equilibrium line  
585 altitude variations of the McKinley River region, central Alaska Range. *Boreas* **39**: 233–246.
- 586 Eynaud F, de Abreu L, Voelker A, Schönfeld J, Salgueiro E, Turon JL, Penaud A, Toucanne S,  
587 Naughton F, Sánchez Goñi MF, Malaizé B, Cacho I. 2009. Position of the Polar Front along the  
588 western Iberian margin during key cold episodes of the last 45 ka. *Geochemistry, Geophysics,*  
589 *Geosystems* **10**.
- 590 Fabel D, Ballantyne CK, Xu S. 2012. Trimlines, blockfields, mountain-top erratics and the vertical  
591 dimensions of the last British- Irish Ice Sheet in NW Scotland. *Quaternary Science Reviews* **55**: 91–102.
- 592 Ffoulkes C, Harrison S. 2014. Evaluating the Schmidt hammer as a method for distinguishing the  
593 relative age of late Holocene moraines: Svellnosbreen, Jotunheimen, Norway. *Geografiska Annaler,*  
594 *Series A: Physical Geography* **96**: 393–402.
- 595 García-Ruiz JM, Gómez-Villar A, Ortigosa L, Martí-Bono C. 2000. Morphometry of glacial cirques in  
596 the Central Spanish Pyrenees. *Geografiska Annaler. Series A, Physical Geography* **82**: 433–442.
- 597 Glasser NF, Hughes PD, Fenton C, Schnabel C, Rother H. 2012. <sup>10</sup>Be and <sup>26</sup>Al exposure-age dating of  
598 bedrock surfaces on the Aran ridge, Wales: evidence for a thick Welsh Ice Cap at the Last Glacial  
599 Maximum. *Journal of Quaternary Science* **27**: 97–104.
- 600 Gosse JC, Phillips FM. 2001. Terrestrial in situ cosmogenic nuclides: theory and application.  
601 *Quaternary Science Reviews* **20**: 1475–1560.

- 602 Hallet B, Putkonen J. 1996. Surface Dating of Dynamic Landforms: Young Boulders on Aging  
603 Moraines. *Science* **265**: 937–940.
- 604 Hambrey MJ, Quincey DJ, Glasser NF, Reynolds JM, Richardson SJ, Clemmens S. 2008.  
605 Sedimentological, geomorphological and dynamic context of debris-mantled glaciers, Mount Everest  
606 (Sagarmatha) region, Nepal. *Quaternary Science Reviews* **27**: 2361–2389.
- 607 Harrison S, Glasser N, Anderson E, Ivy-Ochs, S, Kubik PW. 2010. Late Pleistocene mountain glacier  
608 response to North Atlantic climate change in southwest Ireland. *Quaternary Science Reviews* **29**:  
609 3948-3955.
- 610 Heyman J, Stroeve AP, Harbor JM, Caffee MW. 2010. Too young or too old: Evaluating cosmogenic  
611 exposure dating based on an analysis of compiled boulder exposure ages. *Earth and Planetary Science*  
612 *Letters* **302**: 71–80.
- 613 Hughes PD. 2018. Little Ice Age glaciers and climate in the Mediterranean mountains: A new analysis.  
614 *Cuadernos de Investigación Geográfica* **44**.
- 615 Hughes PD, Braithwaite RJ. 2008. Application of a degree-day model to reconstruct Pleistocene  
616 glacial climates. *Quaternary Research* **69**: 110–116.
- 617 Hughes PD, Gibbard PL. 2015. A stratigraphical basis for the Last Glacial Maximum (LGM).  
618 *Quaternary International* **383**: 174–185.
- 619 Hughes PD, Glasser NF, Fink D. 2016. Rapid thinning of the Welsh Ice Cap at 20-19 ka based on  
620 <sup>10</sup>Be ages. *Quaternary Research* **85**: 107–117.
- 621 Ivy-Ochs S, Kerschner H, Reuther A, Maisch M, Sailer R, Kubik PW, Synal HA, Schlüchter C. 2006.  
622 The timing of glacier advances in the northern European Alps based on surface exposure dating with  
623 cosmogenic <sup>10</sup>Be, <sup>26</sup>Al, <sup>36</sup>Cl, and <sup>21</sup>Ne. In: Siame LL,, In: Bourlès DL,, In: Brown ET, eds. *In Situ–*  
624 *Produced Cosmogenic Nuclides and Quantification of Geological Processes: Geological Society of America*  
625 *Special Paper* **415**. Geological Society of America, 43–60.
- 626 Ivy-Ochs S, Kerschner H, Reuther A, Preusser F, Heine K, Maisch MAX, Kubik PW, Schlüchter C.  
627 2008. Chronology of the last glacial cycle in the European Alps. *Journal of Quaternary Science* **23**: 559–  
628 573.
- 629 Kelly A, Charman DJ, Newnham RM. 2010. A Last Glacial Maximum pollen record from Bodmin  
630 Moor showing a possible cryptic northern refugium in southwest England. *Journal of Quaternary*  
631 *Science* **25**: 296–308.
- 632 Kern Z, László P. 2010. Size specific steady-state accumulation-area ratio: an improvement for  
633 equilibrium-line estimation of small palaeoglaciers. *Quaternary Science Reviews* **29**: 2781–2787.
- 634 Kirkbride MP, Winkler S. 2012. Correlation of Late Quaternary moraines: impact of climate  
635 variability, glacier response, and chronological resolution. *Quaternary Science Reviews* **46**: 1–29.
- 636 Knight JC. 2016. Comment on “Last glacial maximum cirque glaciation in Ireland and implications for  
637 reconstructions of the Irish ice sheet. *Quaternary Science Reviews* 141, 85-93”. *Quaternary Science*  
638 *Reviews* **150**: 308-311.
- 639 Knight L, Boston C, Lovell H, Pepin N. 2017. Last Glacial-Interglacial Transition ice dynamics in the  
640 Wicklow Mountains, Ireland. *Geophysical Research Abstracts* **19**.
- 641 Lal D. 1991. Cosmic ray labeling of erosion surfaces: in situ nuclide production rates and erosion



- 642 models. *Earth and Planetary Science Letters* **104**: 424–439.
- 643 Lloyd JM, Zong Y, Fish P, Innes JB. 2013. Holocene and Lateglacial relative sea-level change in north-  
644 west England: implications for glacial isostatic adjustment models. *Journal of Quaternary Science* **28**:  
645 59–70.
- 646 López-Moreno JI, Nogués-Bravo D, Chueca-Cía J, Julián-Andrés A. 2006a. Glacier development and  
647 topographic context. *Earth Surface Processes and Landforms* **31**: 1585–1594.
- 648 López-Moreno JI, Nogués-Bravo D, Chueca-Cía J, Julián-Andrés A. 2006b. Change of topographic  
649 control on the extent of cirque glaciers since the Little Ice Age. *Geophysical Research Letters* **33**: 1–5.
- 650 Lowe S. 1981. Radiocarbon dating and stratigraphic resolution in Welsh lateglacial chronology.  
651 *Nature* **293**: 210–212.
- 652 Lukas S, Graf A, Coray S, Schlüchter C. 2012. Genesis, stability and preservation potential of large  
653 lateral moraines of Alpine valley glaciers and towards a unifying theory based on Findelengletscher,  
654 Switzerland. *Quaternary Science Reviews* **38**: 27–48.
- 655 Macleod A, Palmer A, Lowe J, Rose J, Bryant C, Merritt J. 2011. Timing of glacier response to  
656 Younger Dryas climatic cooling in Scotland. *Global and Planetary Change* **79**: 264–274.
- 657 Matthews JA, Owen G. 2008. Endolithic lichens, rapid biological weathering and Schmidt Hammer R-  
658 Values on recently exposed rock surfaces: Storbreen glacier foreland, Jotunheimen, Norway.  
659 *Geografiska Annaler, Series A: Physical Geography* **90**: 287–297.
- 660 McCabe AM, Clark PU, Clark J, Dunlop P. 2007. Radiocarbon constraints on readvances of the  
661 British-Irish Ice Sheet in the northern Irish Sea Basin during the last deglaciation. *Quaternary Science*  
662 *Reviews* **26**: 1204–1211.
- 663 McCarroll D, Stone JO, Ballantyne CK, Scourse JD, Fifield LK, Evans DJA, Hiemstra JF. 2010.  
664 Exposure-age constraints on the extent, timing and rate of retreat of the last Irish Sea ice stream.  
665 *Quaternary Science Reviews* **29**: 1844–1852.
- 666 Mills SC, Grab SW, Carr SJ. 2009. Recognition and palaeoclimatic implications of late Quaternary  
667 niche glaciation in eastern Lesotho. *Journal of Quaternary Science* **24**: 647–663.
- 668 Mills SC, Grab SW, Rea BR, Carr SJ, Farrow A. 2012. Shifting westerlies and precipitation patterns  
669 during the Late Pleistocene in southern Africa determined using glacier reconstruction and mass  
670 balance modelling. *Quaternary Science Reviews* **55**: 145–159.
- 671 Mitchell WA. 1996. Significance of snowblow in the generation of Loch Lomond Stadial (Younger  
672 Dryas) glaciers in the western Pennines, northern England. *Journal of Quaternary Science* **11**: 233–248.
- 673 Murari MK, Owen LA, Dortch JM, Caffee MW, Dietsch C, Fuchs M, Haneberg WC, Sharma MC,  
674 Townsend-Small A. 2014. Timing and climatic drivers for glaciation across monsoon-influenced  
675 regions of the Himalayan-Tibetan orogen. *Quaternary Science Reviews* **88**: 159–182.
- 676 Niedzielski T, Migoń P, Placek A. 2009. A minimum sample size required from Schmidt hammer  
677 measurements. *Earth Surface Processes and Landforms* **34**: 1713–1725.
- 678 Ohmura A, Kasser P, Funk M. 1992. Climate at the equilibrium line of glaciers. *Journal of Glaciology* **38**:  
679 397–411.
- 680 Palacios D, García-Ruiz JM, Andrés N, Schimmelpfennig I, Campos N, Léanni L, Team A. 2017.

- 681 Deglaciation in the central Pyrenees during the Pleistocene e Holocene transition: Timing and  
682 geomorphological significance. *Quaternary Science Reviews* **162**: 111–127.
- 683 Pallàs R, Rodés Á, Braucher R, Bourlès D, Delmas M, Calvet M, Gunnell Y. 2010. Small, isolated  
684 glacial catchments as priority targets for cosmogenic surface exposure dating of Pleistocene climate  
685 fluctuations, southeastern Pyrenees. *Geology* **38**: 891–894.
- 686 Pellitero R, Rea BR, Spagnolo M, Bakke J, Hughes P, Ivy-Ochs S, Lukas S, Ribolini A. 2015. A GIS tool  
687 for automatic calculation of glacier equilibrium-line altitudes. *Computers and Geosciences* **82**: 55–62.
- 688 Pellitero R, Rea BR, Spagnolo M, Bakke J, Ivy-Ochs S, Frew CR, Hughes P, Ribolini A, Lukas S,  
689 Renssen H. 2016. GlaRe, a GIS tool to reconstruct the 3D surface of palaeoglaciers. *Computers and*  
690 *Geosciences* **94**: 77–85.
- 691 Putkonen J, Swanson T. 2003. Accuracy of cosmogenic ages for moraines. *Quaternary Research* **59**:  
692 255–261.
- 693 Rae AC, Harrison S, Mighall T, Dawson AG. 2004. Periglacial trimlines and nunataks of the last glacial  
694 maximum: the Gap of Dunloe, Southwest Ireland. *Journal of Quaternary Science* **19**: 87–97.
- 695 Rea BR. 2009. Defining modern day Area-Altitude Balance Ratios (AABRs) and their use in glacier-  
696 climate reconstructions. *Quaternary Science Reviews* **28**: 237–248.
- 697 Reimer PJ, Bard E, Bayliss A, Beck JW, Blackwell PG, Bronk Ramsey C, Buck CE, Cheng H, Edwards  
698 RL, Friedrich M, Grootes PM, Guilderson TP, Haflidason H, Hajdas I, Hatté C, Heaton TJ, Hoffman  
699 DL, Hogg AG, Hughen KA, Kaiser KF, Kromer B, Manning SW, Niu M, Reimer RW, Richards DA,  
700 Scott EM, Southon JR, Staff RA, Turney CSM, van der Plicht J. 2013. Intcal13 and marine13  
701 radiocarbon age calibration curves 0 – 50,000 years cal BP. *Radiocarbon* **55**: 1869–1887.
- 702 Rode M, Kellerer-Pirklbauer A. 2011. Schmidt-hammer exposure-age dating (SHD) of rock glaciers  
703 in the Schöderkogel-Eisenhut area, Schladminger Tauern Range, Austria. *The Holocene* **22**: 761–771.
- 704 Shanahan TM, Zreda M. 2000. Chronology of Quaternary glaciations in East Africa. *Earth and*  
705 *Planetary Science Letters* **177**: 23–42.
- 706 Smedley RK, Chiverrell RC, Ballantyne CK, Burke MJ, Clark CD, Duller GAT, Fabel D, McCarroll D,  
707 Scourse JD, Small D, Thomas GSP. 2017a. Internal dynamics condition centennial-scale oscillations in  
708 marine- based ice-stream retreat. *Geology* **45**: 787–790.
- 709 Smedley RK, Scourse JD, Small D, Hiemstra JF, Duller GAT, Bateman MD, Burke MJ, Chiverrell RC,  
710 Clark CD, Davies SM, Fabel D, Gheorghiu DM, McCarroll D, Medialdea A, Xu S. 2017b. New age  
711 constraints for the limit of the British-Irish Ice Sheet on the Isles of Scilly. *Journal of Quaternary*  
712 *Science* **32**: 48–62.
- 713 Stone JO. 2000. Air pressure and cosmogenic isotope production. *Journal of Geophysical Research* **105**:  
714 23753–23759.
- 715 Sumner P, Nel W. 2002. The effect of rock moisture on Schmidt hammer rebound: Tests on rock  
716 samples from Marion Island and South Africa. *Earth Surface Processes and Landforms* **27**: 1137–1142.
- 717 Svendsen JI, Alexanderson H, Astakhov VI, Demidov I, Dowdeswell JA, Funder S, Gataullin V,  
718 Henriksen M, Hjort C, Houmark-Nielsen M, Hubberten HW. 2004. Late Quaternary ice sheet  
719 history of northern Eurasia. *Quaternary Science Reviews* **23**: 1229–1271.
- 720 Tomkins MD, Dortch JM, Hughes PD. 2016. Schmidt Hammer exposure dating (SHED):

- 721 Establishment and implications for the retreat of the last British Ice Sheet. *Quaternary Geochronology*  
722 **33**: 46–60.
- 723 Tomkins MD, Huck JJ, Dortch JM, Hughes PD, Kirkbride MJ, Barr IB. 2018a. Schmidt Hammer  
724 exposure dating (SHED): Calibration procedures, new exposure age data and an online calculator.  
725 *Quaternary Geochronology* **44**: 55-62.
- 726 Tomkins MD, Dortch JM, Hughes PD, Huck JJ, Stimson AG, Delmas M, Calvet M, Pallàs, R. 2018b.  
727 Rapid age assessment of glacial landforms in the Pyrenees using Schmidt hammer exposure dating  
728 (SHED). *Quaternary Research*. Article In Press.
- 729 Tonkin TN, Midgley NG, Graham DJ, Labadz JC. 2017. Internal structure and significance of ice-  
730 marginal moraine in the Kebnekaise Mountains, northern Sweden. *Boreas* **46**: 199–211.
- 731 Warren CR. 1991. Terminal environment, topographic control and fluctuations of West Greenland  
732 glaciers. *Boreas* **20**: 1–15.
- 733 Williams RBG, Robinson DA. 1983. The effect of surface texture on the determination of the  
734 surface hardness of rock using the Schmidt Hammer. *Earth Surface Processes and Landforms* **8**: 289–  
735 292.
- 736 Wilson P, Schnabel C, Wilcken KM, Vincent PJ. 2013. Surface exposure dating ( $^{36}\text{Cl}$  and  $^{10}\text{Be}$ ) of  
737 post-Last Glacial Maximum valley moraines, Lake District, northwest England: some issues and  
738 implications. *Journal of Quaternary Science* **28**: 379–390.
- 739 Zech R, Glaser B, Sosin P, Kubik PW, Zech W. 2005. Evidence for long-lasting landform surface  
740 instability on hummocky moraines in the Pamir Mountains (Tajikistan) from  $^{10}\text{Be}$  surface exposure  
741 dating. *Earth and Planetary Science Letters* **237**: 453–461.
- 742

## Figures

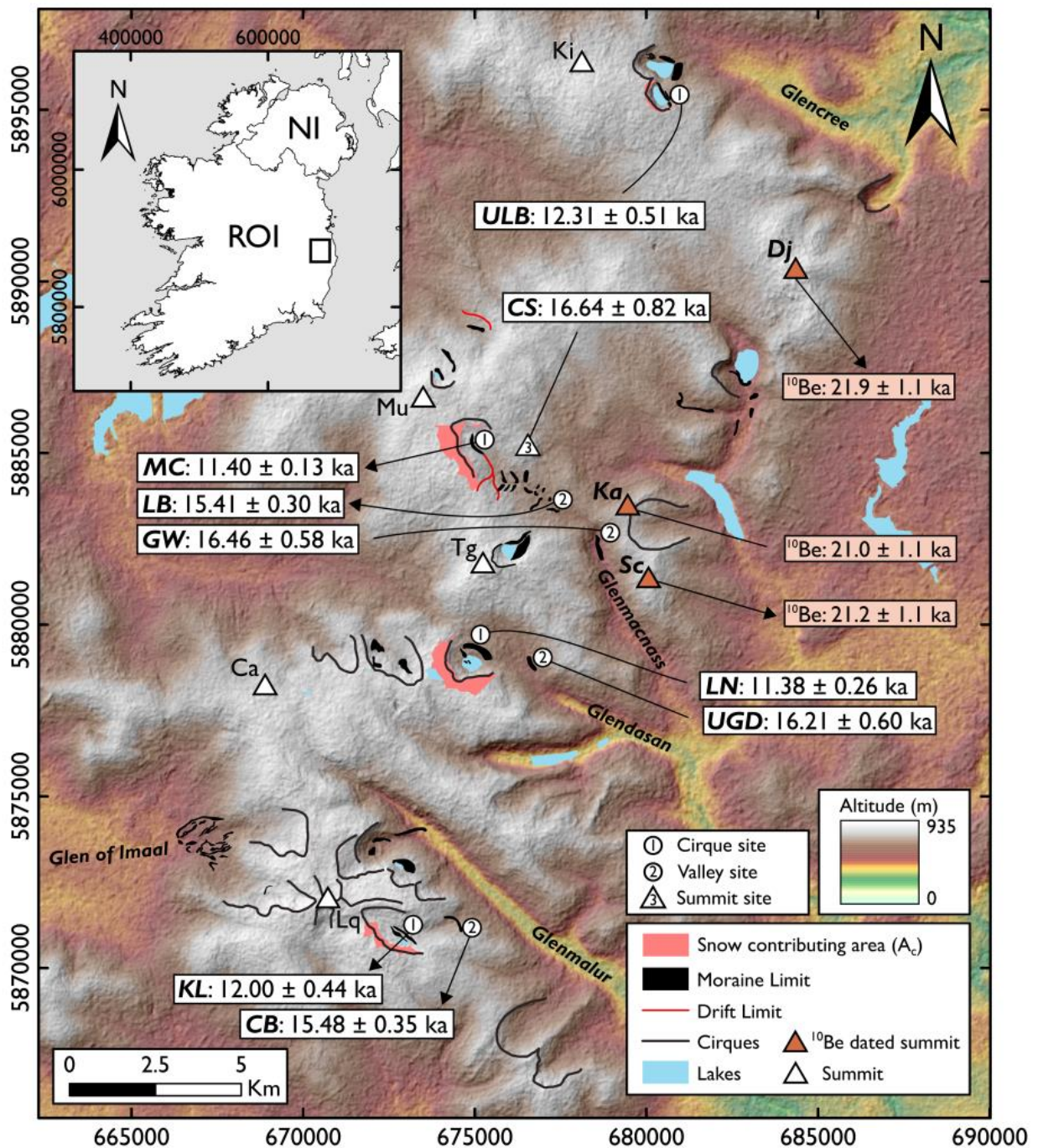


Figure 1. Generalised geomorphological map of the Wicklow Mountains. Moraines modified after Clark et al. (2017).  $^{10}\text{Be}$  ages recalibrated from Ballantyne et al. (2006) using the online calculators formerly known as the CRONUS-Earth online calculator (Wrapper script 2.3, Main calculator 2.1, constants 2.3, muons 1.1; Balco et al., 2008) based on the Loch Lomond Production Rate (Fabel et al., 2012), the time-independent Lm scaling (Lal, 1991; Stone 2000) and assuming 0 mm ka<sup>-1</sup> erosion. Ca: Camenabologue; Dj: Djouce Mountain; Ka: Kanturk; Ki: Kippure; Lq: Lugnaquilla; Mu: Mullaghcleevaun; Sc: Scarr; Tg: Tonelagee. Map projection: UTM WGS 1984.

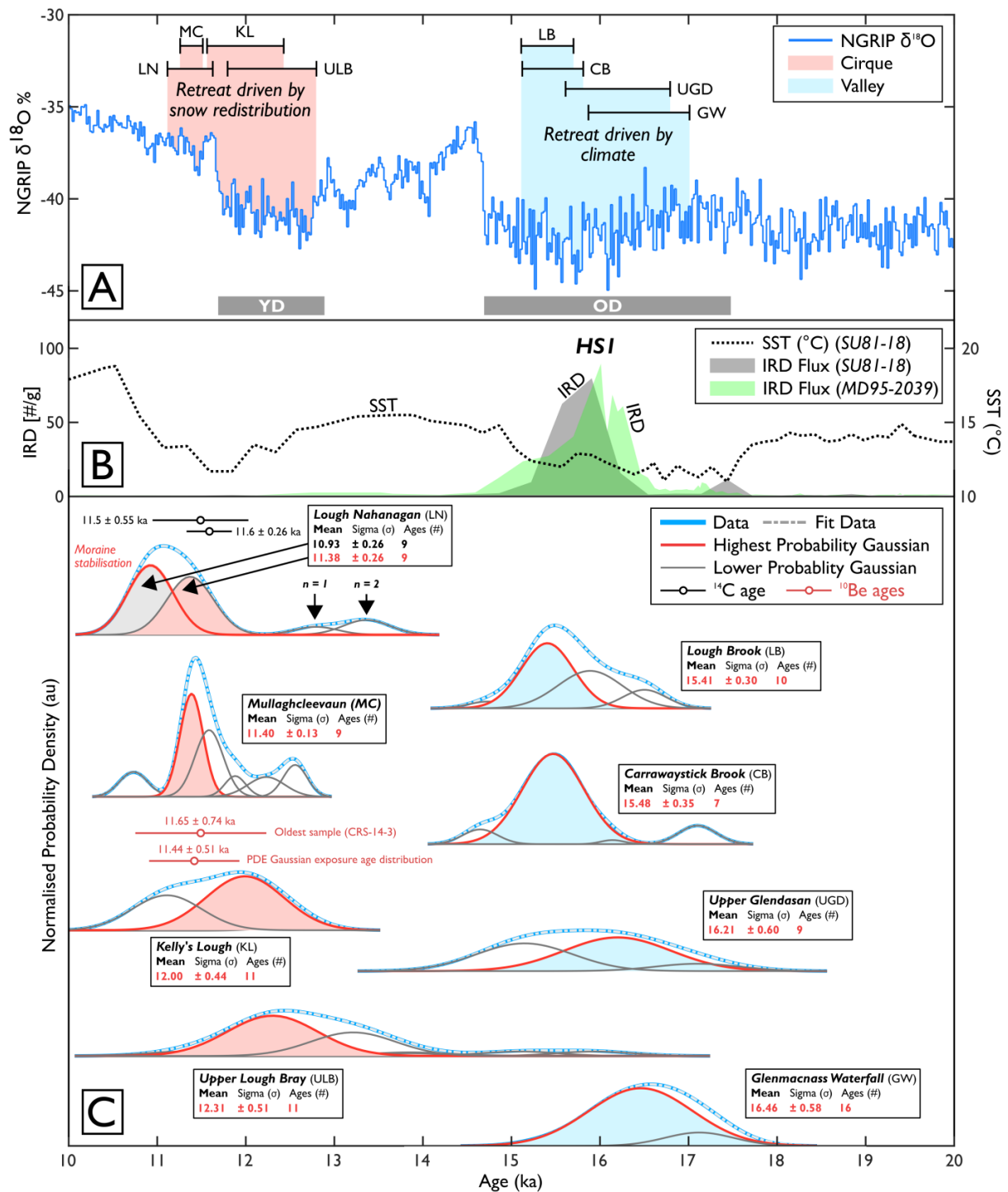


Figure 2. Gaussian ages related to deglaciation of the Wicklow Mountains. A: The NGRIP Oxygen Isotope Curve (Rasmussen et al., 2014) plotted against  $1\sigma$  age boundaries for sampled cirque and valley sites. The Younger Dryas (YD) and Oldest Dryas (OD) periods are marked. B: Ice rafted debris (#/g) and sea surface temperature ( $^{\circ}\text{C}$ ) records from cores SUBI-18 (Bard et al., 2000) and MD95-2039 (Eynaud et al., 2009) in the North Atlantic. C: Gaussian models for sampled cirque and valley sites. For each site, the highest probability Gaussian is considered the most likely timing of deglaciation as all ages are younger than the Last Glacial Maximum (Dortch et al., 2013). At Lough Nahanagan, the oldest peak with more than 3 ages is selected (c.f. Dortch et al., 2013) as this moraine is degraded and morphologically distinct from other sampled cirque moraines (MC, KL, ULB). Moreover, this estimates matches previous  $^{14}\text{C}$  ages (Colhoun and Synge, 1980). At Kelly's

Lough, the peak SHED Gaussian exposure age distribution is matched by independent  $^{10}\text{Be}$  ages (Barth et al., 2018). This estimate overlaps with the peak  $^{10}\text{Be}$  Gaussian exposure age distribution of  $11.44 \pm 0.51$  ka (excluding outlier CRS-14-5d:  $137 \pm 7$  ka) and more conservatively, the oldest sample of  $11.65 \pm 0.74$  ka (CRS-14-3).

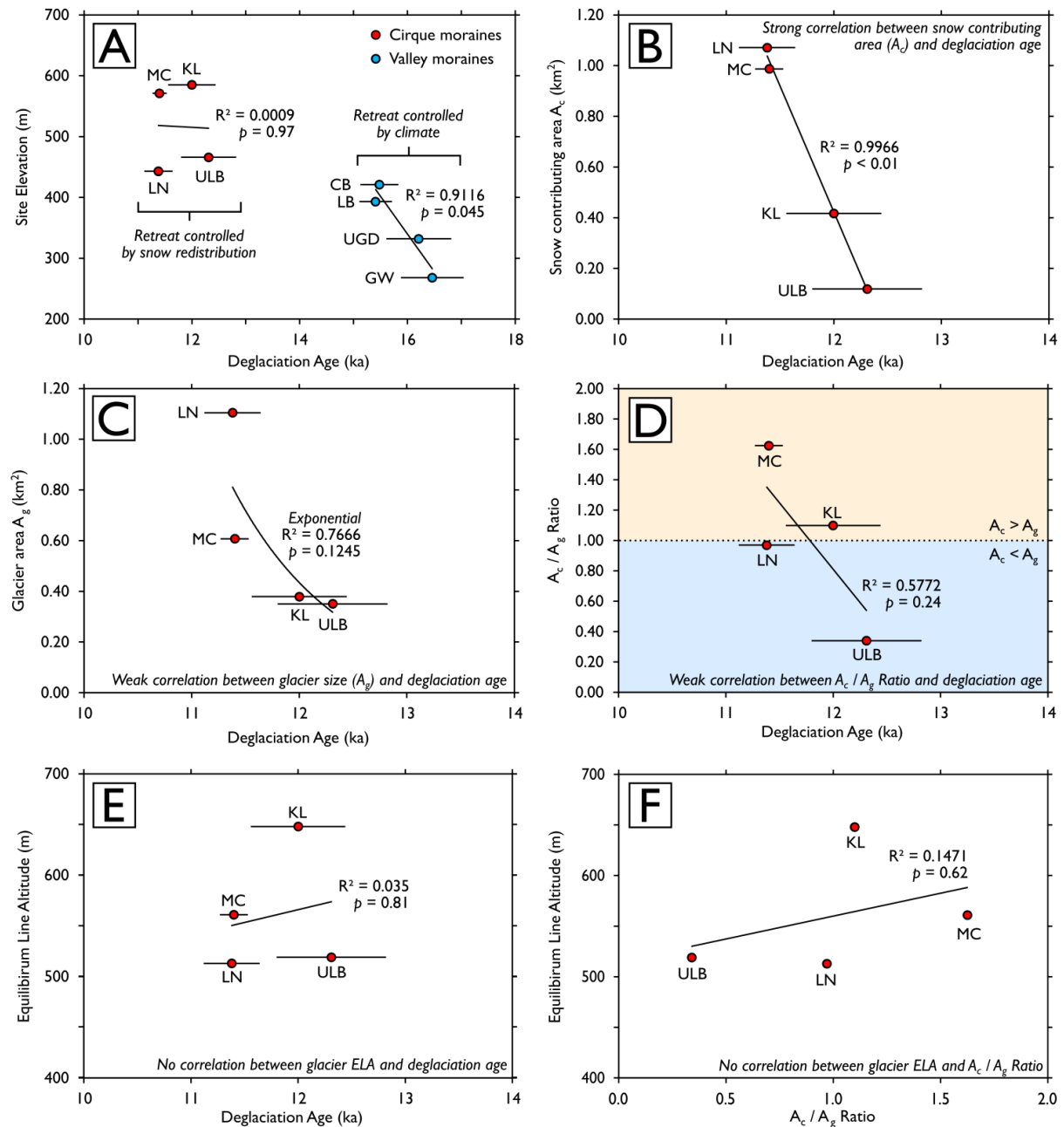


Figure 3. Topographic and climatic controls on the timing of cirque deglaciation in the Wicklow Mountains. A: Site Elevation; B: Snow contributing area ( $A_c$ ); C: Glacier area ( $A_g$ ); D:  $A_c/A_g$  ratio; E: ELA; F: ELAs and  $A_c/A_g$  ratio plots. These data show that for large valley glaciers, retreat is driven by climate with progressive deglaciation from low to high elevation (A). In contrast, marked asynchronicity in the timing of cirque deglaciation (A) is strongly controlled by snow redistribution (B). This asynchronicity is weakly correlated with glacier size (C) and  $A_c/A_g$  ratios (D) and is unrelated to ELA (E).

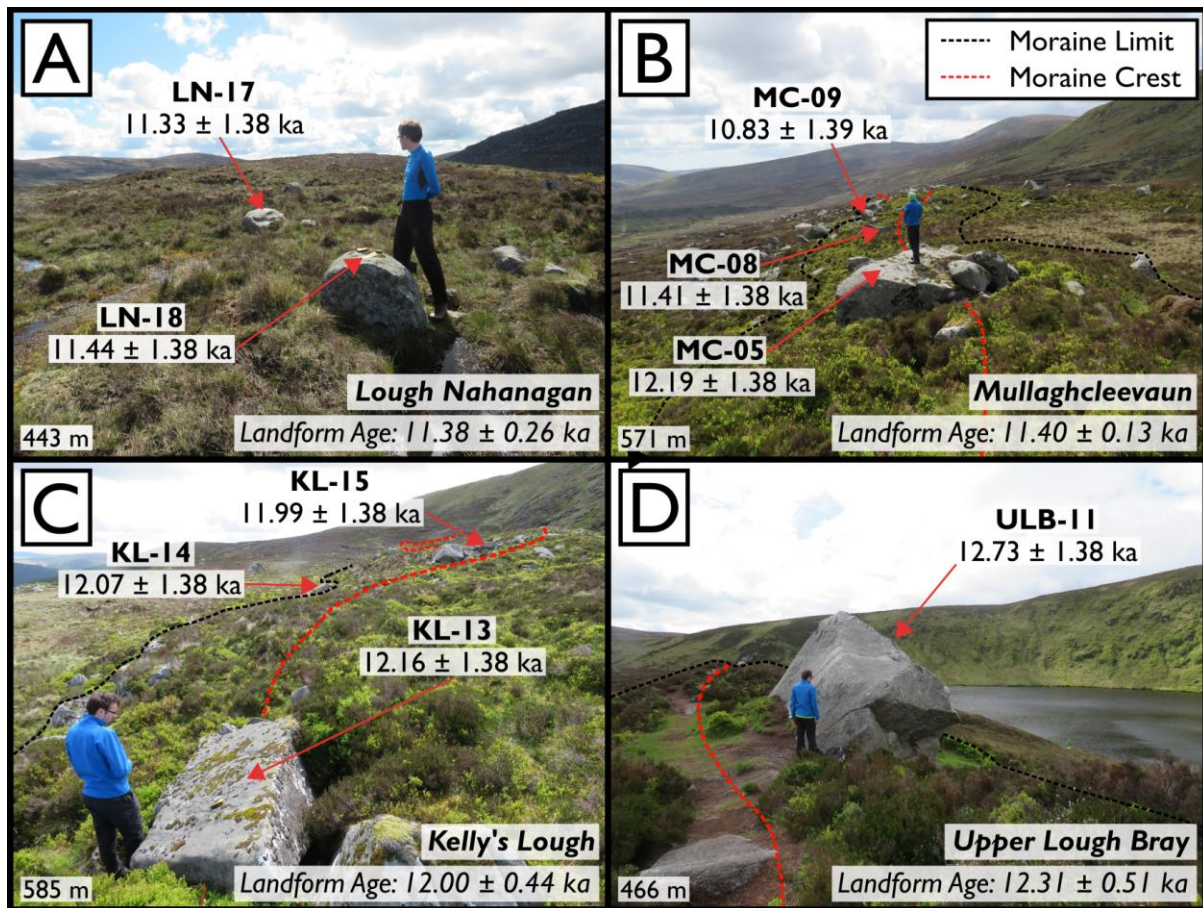


Figure 4. Sampled cirque moraines at Lough Nahanagan (A), Mullaghcleevaun (B), Kelly's Lough (C) and Upper Lough Bray (D). The outer cirque moraine at Lough Nahanagan is degraded (Colhoun and Synge, 1980) and is morphologically distinct from other cirque moraines which are sharp crested, boulder-rich and matrix-poor.

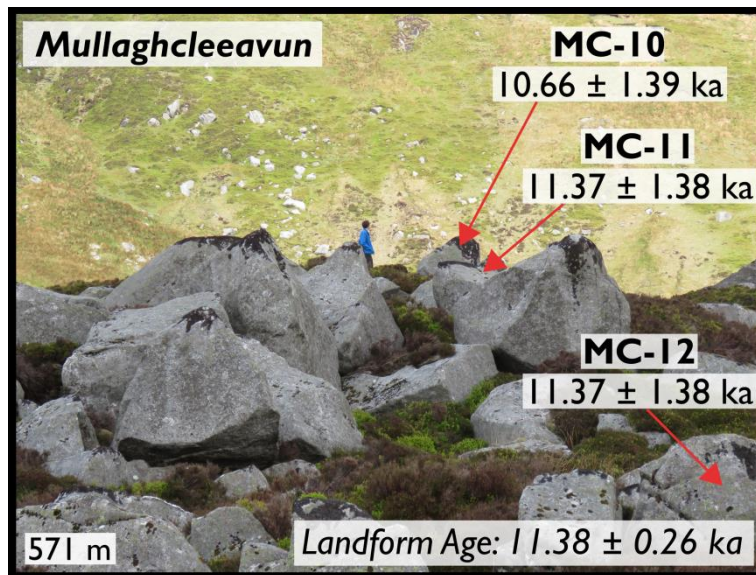


Figure 5. Matrix-poor, boulder-rich moraine at Mullaghcleevun which likely stabilised rapidly after deglaciation.

### Supplementary dataset

Supplementary dataset. Sample information for boulder and bedrock surfaces sampled in the Wicklow Mountains ( $n = 170$ ). Reported R-values are the arithmetic mean of 30 measurements  $\pm$  the standard error of the mean (SEM). Reported ages (ka) were calculated using the SHED-Earth online calculator (<http://shed.earth>; Tomkins et al., 2018a) based on the Loch Lomond Production Rate (LLPR; Fabel et al., 2012), the time-dependent  $L_m$  scaling (Lal, 1991; Stone, 2000) and assuming  $0 \text{ mm ka}^{-1}$  erosion. These numerical ages will be subjected to recalibration in light of future refinement of  $^{10}\text{Be}$  production rates. Available here: [https://www.researchgate.net/publication/325120644\\_Tomkins\\_JOS\\_Supplementary\\_Table](https://www.researchgate.net/publication/325120644_Tomkins_JOS_Supplementary_Table)



## Tables

Table 1. Gaussian ages for cirque, valley and summit sites from the Wicklow Mountains.

Group	Site Name	Site Code	Site Elevation (m)	Site Latitude (°)	Deglaciation Age (ka)	±	Glacier Area ( $A_g$ km <sup>2</sup> )
Cirque	Lough Nahanagan	LN	443	53.034	11.38	0.26	1.10
	Mullaghcleevaun	MC	571	53.089	11.40	0.13	0.61
	Kelly's Lough	KL	585	52.960	12.00	0.44	0.38
	Upper Lough Bray	ULB	466	53.178	12.31	0.51	0.35
Valley	Lough Brook	LB	393	53.070	15.41	0.30	7.63
	Carrawaystick Brook	CB	421	52.964	15.48	0.35	1.83
	Upper Glendasan	UGD	332	53.030	16.21	0.60	4.96
	Glenmacnass Waterfall	GW	268	53.062	16.46	0.58	12.46
Summit	Carrigshouk	CG	571	53.086	16.64	0.82	-

Table 2. Snow contributing areas ( $A_c$ ), glacier areas ( $A_g$ ) and ELAs for cirque moraines.

Site Code	Deglaciation Age (ka)	$\pm$	Snow Contributing Area ( $A_c$ km <sup>2</sup> ) <sup>a</sup>	Glacier Area ( $A_g$ km <sup>2</sup> )	$A_c / A_g$ Ratio	ELA <sup>b</sup>
LN	11.38	0.26	1.07	1.10	0.97	513
MC	11.40	0.13	0.99	0.61	1.62	561
KL	12.00	0.44	0.42	0.38	1.10	648
ULB	12.31	0.51	0.12	0.35	0.34	519

<sup>a</sup> Area within the glacier drainage basin within the 210 – 300° quadrant + all other slopes which overlook the glacier (Gradients > 25°), <sup>b</sup> AABR = 1.9 ± 0.81 (Rea, 2009)

